Journal of
Medical Genetics

# A novel mutation in the GFAP gene expands the phenotype of Alexander Disease

| | |
|---|---|
| Journal: | *Journal of Medical Genetics* |
| Manuscript ID | jmedgenet-2018-105959.R1 |
| Article Type: | Short Report |
| Date Submitted by the Author: | n/a |
| Complete List of Authors: | Casasnovas, Carlos; Hospital Universitari de Bellvitge, Neurology; Institut d'Investigacio Biomedica de Bellvitge, Neurometabolic Disease Lab<br>Verdura, Edgard; Institut d'Investigacio Biomedica de Bellvitge, Neurometabolic Disease Lab<br>Vélez, Valentina; Hospital Universitari de Bellvitge, Neurology; Institut d'Investigacio Biomedica de Bellvitge, Neurometabolic Disease Lab<br>Schlüter, Agatha; Institut d'Investigacio Biomedica de Bellvitge, Neurometabolic Disease Lab<br>Pons-Escoda, Albert; Hospital Universitari de Bellvitge, Neuroradiology<br>Homedes, Christian; Hospital Universitari de Bellvitge, Neurology<br>Ruiz, Montserrat; Institut d'Investigacio Biomedica de Bellvitge, Neurometabolic Disease Lab<br>Fourcade, Stéphane; Institut d'Investigacio Biomedica de Bellvitge, Neurometabolic Disease Lab<br>Launay, Nathalie; Institut d'Investigacio Biomedica de Bellvitge, Neurometabolic Disease Lab<br>Pujol, Aurora; Institut d'Investigacio Biomedica de Bellvitge, Neurometabolic Disease Lab |
| Keywords: | GFAP, Alexander disease, WES, astrocyte hypertrophy |
| | |

Note: The following files were submitted by the author for peer review, but cannot be converted to PDF. You must view these files (e.g. movies) online.

Supplementary File – Video. Presence of mild abnormalities in ocular movements (nistagmus) in patient III.5 (paucisintomatic).mp4

# A novel mutation in the *GFAP* gene expands the phenotype of Alexander Disease

Carlos Casasnovas,[1,2,3] Edgard Verdura,[1,3] Valentina Vélez-Santamaria,[1,2] Agatha Schlüter,[1,3] Albert Pons-Escoda,[4] Christian Homedes,[2] Montserrat Ruiz,[1,3] Stéphane Fourcade,[1,3] Nathalie Launay,[1,3] Aurora Pujol,[1,3,5]

1- Neurometabolic Diseases Laboratory, Bellvitge Biomedical Research Institute (IDIBELL), L'Hospitalet de Llobregat, Barcelona, Spain

2- Neuromuscular Unit, Neurology Department, Hospital Universitari de Bellvitge, L'Hospitalet de Llobregat, Barcelona, Spain

3- Centre for Biomedical Research on Rare Diseases (CIBERER), Instituto de Salud Carlos III, Spain.

4- Neuroradiology Unit, Institut de Diagnòstic per la Imatge-IDI, Hospital Universitari de Bellvitge, L'Hospitalet de Llobregat, Spain

5- Catalan Institution of Research and Advanced Studies (ICREA), Barcelona, Catalonia, Spain

CC and EV contributed equally to this manuscript.

Correspondence should be addressed to: Professor Aurora Pujol, Neurometabolic Diseases Laboratory, IDIBELL, Hospital Duran i Reynals, Gran Via 199, 08908 L'Hospitalet de Llobregat, Barcelona, Spain. Tel: +34 932607137; Fax: +34 932607414; Email: apujol@idibell.cat

**Manuscript word count (excluding title page, abstract, references, figures and tables):** 1978 words

## ABSTRACT

**Background**: Alexander disease, an autosomal dominant leukodystrophy, is caused by missense mutations in *GFAP*. Although mostly diagnosed in children, associated with severe leukoencephalopathy, milder adult forms also exist.

**Methods**: A family affected by adult-onset spastic paraplegia underwent neurological examination and cerebral MRI. Two patients were sequenced by WES. A candidate variant was functionally tested in an astrocytoma cell line.

**Results**: The novel variant in GFAP N-terminal head domain (p.Gly18Val) cosegregated in multiple relatives (LOD score: 2.7). All patients, even those with the mildest forms, showed characteristic signal changes or atrophy in the brainstem and spinal cord MRIs, and abnormal MRS. *In vitro*, this variant did not cause significant protein aggregation, in contrast to most Alexander disease mutations characterized so far. However, cell area analysis showed larger size, a feature previously described in patients and mouse models.

**Conclusion**: We suggest that this variant causes variable expressivity and an attenuated phenotype of Alexander Disease type II, probably associated with alternative pathogenic mechanisms, i.e. astrocyte enlargement. *GFAP* analysis should be considered in adult-onset neurologic presentations with pyramidal and bulbar symptoms, in particular when characteristic findings, such as the tadpole sign, are present in MRI. WES is a powerful tool to diagnose atypical cases.


**Keywords:** “Alexander disease”, “GFAP”, “WES”, “astrocyte hypertrophy”

## INTRODUCTION

Missense gain-of-function mutations in *GFAP* are the only known cause of Alexander disease, a rare neurodegenerative disorder pathologically defined by white matter degeneration and the presence of characteristic Rosenthal fibres (intracytoplasmic inclusions in astrocytes).[1, 2] In infantile cases (Alexander Disease type I), patients present developmental delay, macrocephaly, seizures and progressive encephalopathy, leading to death within the first decade. MRI shows leukoencephalopathy without brainstem abnormalities.[3] Later-onset cases (Alexander Disease type II) present wide phenotypic variability, with symptoms such as ataxia, spastic paraparesis, palatal tremor, abnormal ocular movements, and bulbar or pseudobulbar symptoms.[4] Additional neurologic signs such as dysautonomia, urinary disturbances and sleep disorders are often described.[5] Atypical features, including scoliosis, mild cognitive deficit, parkinsonism, seizures, peripheral neuropathy or microcoria, have been reported.[6-8] MRI shows little cerebral white matter involvement and is characterized by atrophy and signal intensity changes in the brainstem.[9]

Although most *GFAP* mutations occur *de novo,* adult-onset Alexander disease has also been described in familial cases with autosomal dominant transmission.[7] In this work, we report a family affected by ocular movement abnormalities and mild signs of pyramidal involvement, in which a rare variant of the *GFAP* gene was found by whole exome sequencing (WES). Based on clinical data and functional studies, we suggest that this variant is less deleterious than the vast majority of Alexander disease mutations, giving rise to an attenuated clinical phenotype.

## RESULTS

A 46-year-old Caucasian woman (Figure 1, patient II:3) presented with a 2-year history of spasticity and lower limb weakness. Cranial and cervical MRI was initially reported as normal. She denied a history of neurological disease in her family, except for a maternal cousin (patient II:5), who had "gait problems". She also mentioned that her 16-year-old son (patient III:4) had

frequent falls and mild difficulties in running starting at 9 years old, similar to her cousin's son (patient III:5). After ruling out acquired causes we tested spastic paraparesis genes (SPG3, SPG4, SPG10 and SPG11) and *ABCD1* gene (X-linked adrenomyeloneuropathy), with negative results. Genetic tests for hereditary ataxias were also negative. In a final attempt to elucidate this disease, we included the family in a research protocol and carried out WES on patients II:5 and III:4. WES analysis revealed 5 rare variants shared by both patients. Only one variant cosegregated in all 4 affected relatives (II:3, II:5, III:4 and III:5); an heterozygous missense variant in the *GFAP* gene, p.Gly18Val. Mutations in this gene cause Alexander disease (OMIM #203450), an autosomal dominant leukodystrophy with described adult presentations.[1, 4] This variant was not previously associated with Alexander disease, nor was it present in databases of control individuals (1000 Genomes, ExAC, and gnomAD). Segregation analysis indicated that this variant was also carried by two asymptomatic family members (I:2 and II:2). We therefore decided to clinically re-evaluate all family members and found abnormalities in ocular movements and pyramidal involvement in both two patients. In conclusion, this family showed variable disease expressivity among 4 patients exhibiting clear signs of disease and 2 paucisymptomatic individuals who presented alterations in neurological examination but had no complaints nor symptoms (patients I:2 and II:2). The age of clinical onset ranged from 9 to 46 years, and age at diagnosis ranged from 16 to 73 years. Clinical findings are summarized in Supplemental Table 1, and Supplemental Video 1 shows movement abnormalities in patient III:5.

In patients II:3, II:5, III:4 and III:5, symptoms at disease onset included asymmetric proximal lower limb weakness due to pyramidal involvement, which was associated with proximal upper limb weakness in patient II:5. All four subjects had gait difficulties due to spastic paraparesis. Patients II:3 and II:5, aged 49 and 48 years old at first examination, needed unilateral support to walk. Patients II:3 and II:5 referred urinary disturbances; urodynamic study of patient II:3 confirmed detrusor overactivity. All patients showed abnormalities in ocular movement, with gaze-evoked nystagmus without ptosis, diplopia or alterations in saccadic pursuit; brisk tendon

reflexes/hyperreflexia; extensor plantar responses; and Hoffman sign. Patients II:2, II:3, III:4 and III:5 presented mild scoliosis.

An exhaustive MRI re-evaluation of patient II:3 revealed signal changes and medullar atrophy. Brain and spinal cord MRI study were then extended to patients II:2, II:5, III:4 and III:5. All patients showed a mild signal change in T2/FLAIR sequences in the brainstem, specifically in the medulla and cervical spinal cord. This is illustrated by MRI images of patient II:3, in which signal change is visible in midbrain (Figure 1B), medulla (Figure 1C) and the spinal cord (Figure 1D). Furthermore, patients II:3, II:5, III:4 and III:5 showed the characteristic "tadpole sign": some degree of atrophy of the cerebellum, medulla and spinal cord with a well-preserved pontine base, markedly characteristic of Alexander disease (illustrated in Figure 1E).[10] The paucisymptomatic Patient II:2, had no atrophy, nor tadpole sign, but showed signal change in the medulla and spinal cord (Figure 1F, 1G). MR Spectroscopy was carried out in patients II.2, II.3, II.5, and III.4, with voxels centered in the area of signal and morphologic abnormality. All patients showed highly elevated levels of myo-inositol and choline with a decreased total *N*-acetyl-aspartate in the ponto-medullary junction (Figure 1H, 1I, Supplemental Figure 1), a feature described in Alexander Disease.[11,12] Radiological findings are summarized in Supplemental Table 2 and illustrated in Figure 1 and Supplemental Figure 1.

This *GFAP* gene variant (chr17:42992802C>A GRCh37; NM_001131019: c.53G>T; p.Gly18Val), found in all affected family members, was located in GFAP's N-terminal head domain, which plays an important role in self-assembly process.[13] This is the most N-terminal variant ever described. However, this residue is not strongly conserved in evolution, missense predictors were not conclusive, and no other pathogenic variants are known in the vicinity. When considering all genotyped individuals, this variant reached a maximum LOD score of 2.7 (odds of ~500 to 1 supporting linkage of this locus to the disease). By applying the American College of Medical Genetics (ACMG) criteria for variant interpretation to assess this nucleotide change[14], we reached a classification of VUS (Variant of Unknown Significance), and thus decided to functionally validate this variant using a transfection assay to test the capacity of the

GFAP protein carrying p.Gly18Val to induce protein aggregation in the astrocytoma cell line U251-MG (Supplemental methods).[15, 16] We utilized two GFAP-EGFP control constructs, one containing the wild-type GFAP sequence, and the second incorporating the p.Arg239Cys mutation, a widely used positive control for GFAP protein aggregation. As described elsewhere, transfection of the WT construct showed large inclusions in ~20% of transfected cells[17, 18], both after 24h or 48h of transfection. Cells transfected with the p.Arg239Cys-mutated construct showed the same large inclusions, but also dot-like clumps or aggregates, as reported [15, 16], which in some cases were distributed around the cell and in other cases converged and formed large aggregates near the cell nucleus, in particular at 48h after transfection (Figure 2A). In contrast, after transfecting the p.Gly18Val-mutant construct we did not observe aggregates similar to the p.Arg239Cys construct, but rather, cells showed an aspect comparable to WT cells, but with lesser inclusions (Supplemental Figure 2A, 2B). This effect was more clear at shorter transfection times (24h) or lower amounts of construct (1µg) (Figure 2A). Interestingly, in the p.Gly18Val condition we observed abnormally large cell sizes, with long astrocytic processes, a phenotype which was confirmed by quantitative image analysis (Figure 2B).

## DISCUSSION

We present a family affected by a dominantly inherited neurological disease, characterized by mild to moderate late-onset cerebellar and pyramidal signs, showing signal abnormalities or atrophy in the brainstem and spinal cord, in whom we identified a candidate variant in *GFAP* using WES, segregating even in asymptomatic individuals. Clinical re-evaluation of all family members combined with functional validation of the novel variant ultimately led to a definitive diagnosis of familial Alexander disease type II.

Clinically, Alexander disease type II presents with cerebellar ataxia, pyramidal involvement, bulbar symptoms and palatal tremor. It is accompanied by variable MRI findings, although most cases present the "tadpole sign" .[10] In this family, four patients showed clear signs of cerebellar dysfunction, with mild ataxia, alteration of ocular movements and spastic paraparesis with

hyperreflexia and extensor plantar responses, and two patients were paucisymptomatic, presenting mild alterations in neurological examination, namely, scoliosis, nystagmus, diplopia, hyperreflexia and the Babinski sign. MRI images of all symptomatic patients showed notable atrophy of the spinal cord and medulla, in contrast to what was observed in the less affected patients, who presented mild signal changes in the trunk and less atrophy. We nonetheless wish to emphasize that all patients except one (patient II:2) presented the previously mentioned tadpole sign. Moreover, MRS on patients II.2, II.3, II.5, and III.4 showed a metabolite profile suggesting hypertrophy of astrocytes as previously discussed [11], consistent with neuroaxonal degeneration.[12] This underscores our *in vitro* findings showing size enlargement of astrocytes.

Indeed, no dot-like clumps or protein aggregates were found for the p.Gly18Val GFAP construct in our functional study, in contrast to most other pathogenic variants described in the literature.[7,15] We also detected lesser inclusions than the WT construct, in particular when transfected with lesser amounts of plasmid. However, we detected an increased size in p.Gly18Val-transfected cells when compared to the WT and p.Arg239Cys constructs. Astrocyte hypertrophy is a known consequence of *GFAP* mutations in Alexander disease, as observed in mouse models and patient's necropsies.[19, 20] It is possible that astrocyte hypertrophy has been historically overlooked for other mutations *in vitro* due to the strong specificity of GFAP aggregates. We thus propose considering astrocyte hypertrophy as an additional criterion of pathogenicity in the functional evaluation of unreported variants.

Although we did not have access to brain biopsies from these patients, the absence of strong pathological signs in MRI and milder clinical manifestations in this family are compatible with the results of the aggregation assay for p.Gly18Val. This expansion of the clinical spectrum of Alexander disease suggests that other adult-onset neurologic cases with overlapping ataxia and pyramidal involvement may be caused by pathogenic *GFAP* variants. Therefore, screening of this gene would be recommended in presence of those symptoms and abnormal findings in MRI, even when these are subtle. An exhaustive and systematic clinical exploration of family members with milder forms or an absence of overt symptoms is recommended, since it may

lead to the identification of clinically unnoticed cases. This work underscores the usefulness of WES to identify paucisymptomatic or atypical cases, and proposes its implementation as first-tier test for neurogenetic conditions with adult presentations, with the goal of improving disease management and genetic counselling.

**Acknowledgements**

We thank CERCA Program/ Generalitat de Catalunya for institutional support. We also thank Juanjo Martínez, Cristina Guilera and Laia Grau for excellent technical assistance and Asociación Española contra las Leucodistrofias (ALE-ELA España).

**Contributors**

CC, EV, SF and AP designed and conceptualized the study. CC, EV, VV, AS, APE, CH, MR, and NL analysed and interpreted the data. CC, EV, VV and AP drafted the manuscript. All authors critically revised the manuscript.

**Funding**

This study was supported by the Centre for Biomedical Research on Rare Diseases (CIBERER) [ACCI14-759], Hesperia Foundation and the Secretariat for Universities and Research of the Ministry of Business and Knowledge of the Government of Catalonia [2017SGR1206] to AP, and Instituto de Salud Carlos III [PI14/00581] (Co-funded by European Regional Development Fund. ERDF, a way to build Europe) and la Marató de TV3 [345/C/2014] to CC. EV was funded by a grant of Ministerio de Economia, Industria y Competividad (Juan de la Cierva programme FJCI-2016-28811); SF was funded by Instituto de Salud Carlos III [Miguel Servet programme CPII16/00016] and MR and NL were funded by CIBERER.

**Competing interests**

The authors report no disclosures or conflicts of interest relevant to the manuscript.

**Patient consent**

Informed consent was obtained from all participants in this study.

**Ethics approval**

The research project was approved by the Clinical Research Ethics Commitee for Research Ethics Committee of the Bellvitge University Hospital (PR076/14).

**Provenance and peer review**

Not commissioned; externally peer reviewed.

**Data sharing statement**

All data are in the submitted paper.

## References

1. Brenner M, Johnson AB, Boespflug-Tanguy O, *et al.* Mutations in GFAP, encoding glial fibrillary acidic protein, are associated with Alexander disease. *Nat Genet* 2001;**27**(1):117-20.
2. Messing A, Brenner M, Feany MB, *et al.* Alexander disease. *J Neurosci* 2012;**32**(15):5017-23.
3. van der Knaap MS, Naidu S, Breiter SN, *et al.* Alexander disease: diagnosis with MR imaging. *AJNR Am J Neuroradiol* 2001;**22**(3):541-52.
4. Pareyson D, Fancellu R, Mariotti C, *et al.* Adult-onset Alexander disease: a series of eleven unrelated cases with review of the literature. *Brain* 2008;**131**(Pt 9):2321-31.
5. Balbi P, Salvini S, Fundaro C, *et al.* The clinical spectrum of late-onset Alexander disease: a systematic literature review. *J Neurol* 2010;**257**(12):1955-62.
6. Brockmann K, Meins M, Taubert A, *et al.* A novel GFAP mutation and disseminated white matter lesions: adult Alexander disease? *Eur Neurol* 2003;**50**(2):100-5.
7. Li R, Johnson AB, Salomons G, *et al.* Glial fibrillary acidic protein mutations in infantile, juvenile, and adult forms of Alexander disease. *Ann Neurol* 2005;**57**(3):310-26.
8. Sreedharan J, Shaw CE, Jarosz J, *et al.* Alexander disease with hypothermia, microcoria, and psychiatric and endocrine disturbances. *Neurology* 2007;**68**(16):1322-3.
9. Graff-Radford J, Schwartz K, Gavrilova RH, *et al.* Neuroimaging and clinical features in type II (late-onset) Alexander disease. *Neurology* 2014;**82**(1):49-56.
10. Namekawa M, Takiyama Y, Honda J, *et al.* Adult-onset Alexander disease with typical "tadpole" brainstem atrophy and unusual bilateral basal ganglia involvement: a case report and review of the literature. *BMC Neurol* 2010;**10**:21.
11. van der Voorn JP, Pouwels PJ, Salomons GS, *et al.* Unraveling pathology in juvenile Alexander disease: serial quantitative MR imaging and spectroscopy of white matter. *Neuroradiology* 2009;**51**(10):669-75.
12. Brockmann K, Dechent P, Meins M, *et al.* Cerebral proton magnetic resonance spectroscopy in infantile Alexander disease. *J Neurol* 2003;**250**(3):300-6.
13. Inagaki M, Nakamura Y, Takeda M, *et al.* Glial fibrillary acidic protein: dynamic property and regulation by phosphorylation. *Brain Pathol* 1994;**4**(3):239-43.
14. Richards S, Aziz N, Bale S, *et al.* Standards and guidelines for the interpretation of sequence variants: a joint consensus recommendation of the American College of Medical Genetics and Genomics and the Association for Molecular Pathology. *Genet Med* 2015;**17**(5):405-24.
15. Bachetti T, Caroli F, Bocca P, *et al.* Mild functional effects of a novel GFAP mutant allele identified in a familial case of adult-onset Alexander disease. *Eur J Hum Genet* 2008;**16**(4):462-70.
16. Yoshida T, Sasayama H, Nakagawa M. The process of inducing GFAP aggregates in astrocytoma-derived cells is different between R239C and R416W mutant GFAP. A time-lapse recording study. *Neurosci Lett* 2009;**458**(1):11-4.
17. Koyama Y, Goldman JE. Formation of GFAP cytoplasmic inclusions in astrocytes and their disaggregation by alphaB-crystallin. *Am J Pathol* 1999;**154**(5):1563-72.
18. Moeton M, Stassen OM, Sluijs JA, *et al.* GFAP isoforms control intermediate filament network dynamics, cell morphology, and focal adhesions. *Cell Mol Life Sci* 2015;**73**(21):4101-20.
19. Sosunov A, Olabarria M, Goldman JE. Alexander disease: an astrocytopathy that produces a leukodystrophy. *Brain Pathol* 2018;**28**(3):388-398.
20. Sosunov AA, Guilfoyle E, Wu X, *et al.* Phenotypic conversions of "protoplasmic" to "reactive" astrocytes in Alexander disease. *J Neurosci* 2013;**33**(17):7439-50.

## LEGENDS

**Figure 1: Family tree and genotype data for the p.Gly18Val variant and brain and cervical MRI and MRS of patients II.3 and II:2.**

(A) Family tree and genotype data for the p.Gly18Val variant. Square: male; circle: female; diagonal black line:deceased; black-filled symbol: affected individual; white-filled symbol: clinically healthy; question mark: unknown status; syringe symbol: blood sampled individual; asterisk: individual sequenced by Whole Exome Sequencing (WES). p.Gly18Val/+ stands for the presence of the p.Gly18Val variant in the heterozygous state, +/+ stands for the absence of this variant in the studied individual. (B-E): Brain MRI images of patient II:3, symptomatic. (B-C): Axial fluid-attenuated inversion recovery (FLAIR) shows signal change in midbrain (B, arrow) and Subpial enhacement in medulla (C, arrow). (D): Sagittal fluid-attenuated inversion recovery (FLAIR) sequence shows spinal cord signal change and atrophy. (E): T1-weighted sagittal section shows the typical tadpole sign, with mild atrophy of medulla and cervical spinal cord and sparing the pons. (F-G): Brain MRI of patient II:2, paucisymptomatic, who presents with subtile signs of piramidal and bulbar involvement but no complaints. (F): Sagittal fluid-attenuated inversion recovery (FLAIR) sequence and (G): Sagittal T2-weighted sequence show absence of atrophy of the brainstem, but demonstrates spinal cord signal change. (H-I): Mean spectra of Proton MRS of Patients II:2, II:3, II:5, III:4 in the medulla-cord junction, at short (30ms, Image H) and long (136ms, Image I) TE. Images show high myoinositol (MYO) and choline (CHO) in contrast to low N-acetylaspartate (NAA).

**Figure 2: Absence of aggregates and cell area enlargement in GFAP-EGFP$^{Gly18Val}$-transfected U251-MG cells**.

A) Images showing transfected U251-MG cells. Green: EGFP fluorescence; red: GFAP; yellow: merged images showing colocalization with EGFP and GFAP in transfected cells. Blue indicates DAPI staining. In the second column, magnifications are shown in the lower right corner. B) Representative confocal microscopy images (63x) show U251-MG astrocytoma cells

transfected with vectors expressing GFAP-EGFP$^{WT}$, GFAP-EGFP$^{Arg239Cys}$, or GFAP-EGFP$^{Gly18Val}$. In the p.Gly18Val image, two representative enlarged transfected cells are shown. The cell area of the transfected cells is shown as a box plot. Error bars indicate the standard deviations of two independent experiments. ***, $p<0.001$. Green: GFAP-EGFP; blue: DAPI; yellow outlining: area considered for cell area measurement.

**Supplemental Material Video 1:** Presence of mild abnormalities in ocular movements (nystagmus) in patient III:5 (paucisymptomatic).

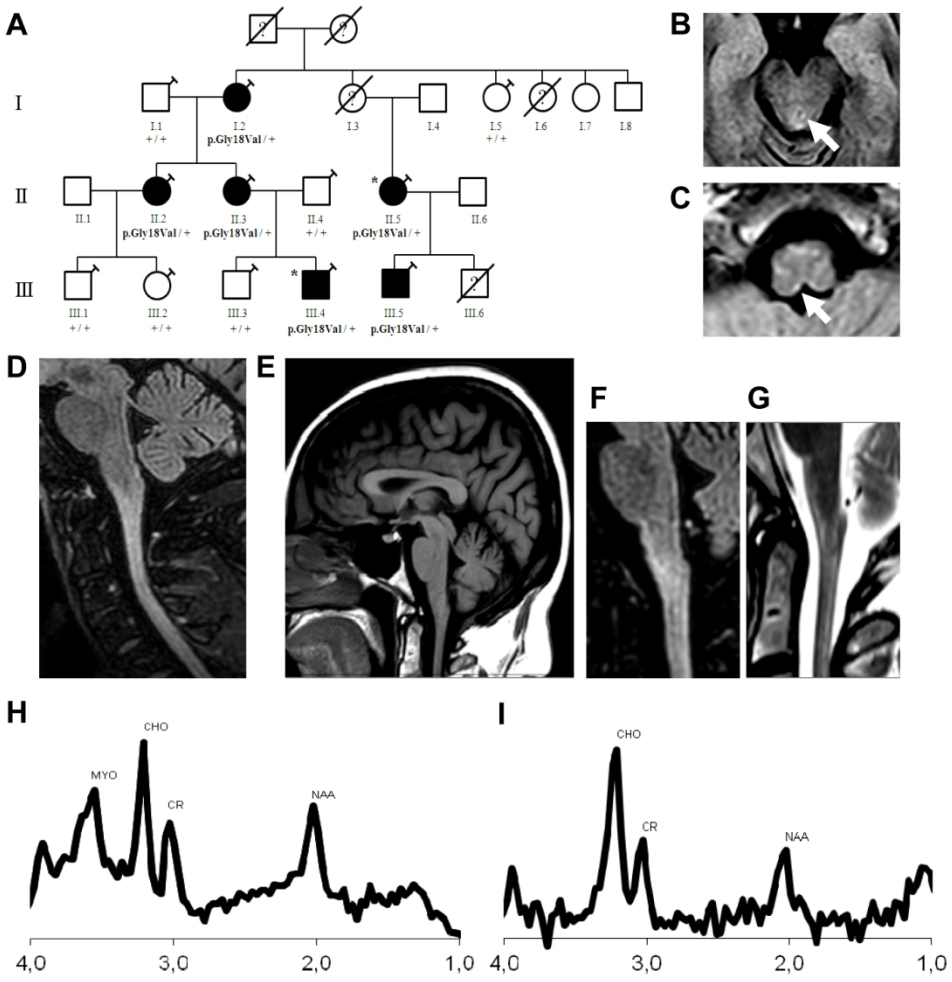


Figure 1: Family tree and genotype data for the p.Gly18Val variant and brain and cervical MRI and MRS of patients II.3 and II:2.

162x162mm (300 x 300 DPI)

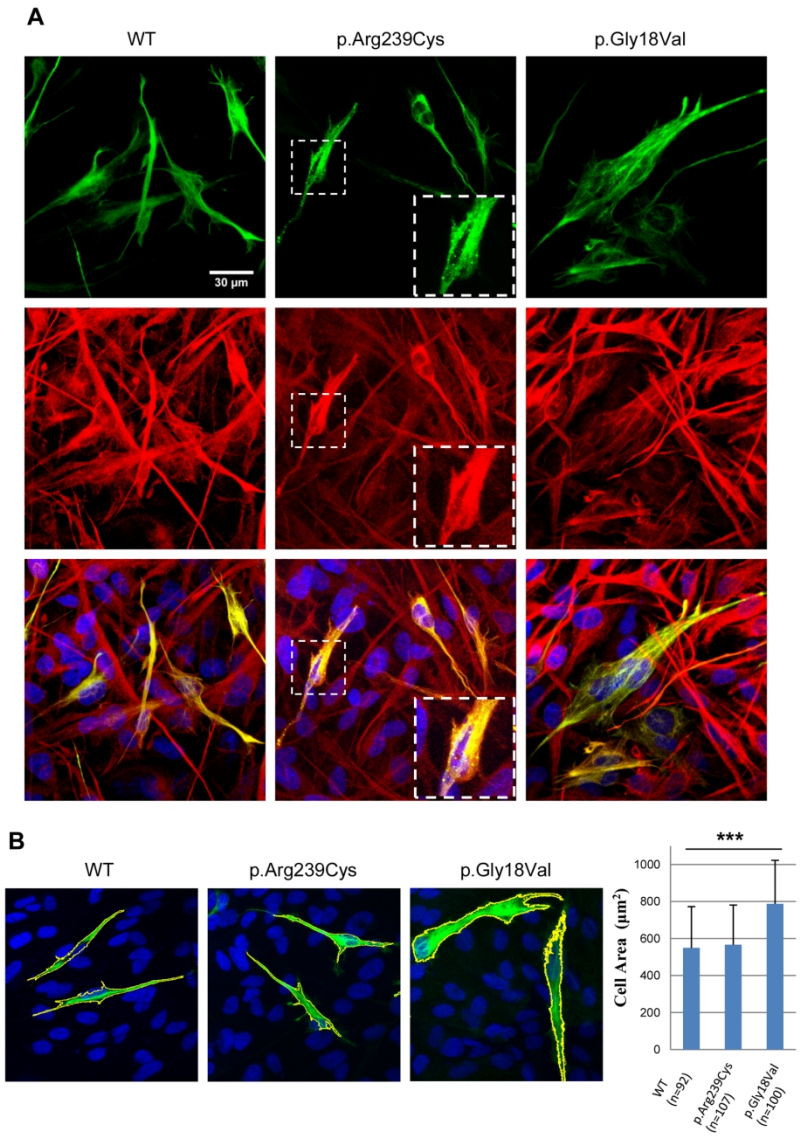


Figure 2: Absence of aggregates and cell area enlargement in GFAP-EGFPGly18Val-transfected U251-MG cells.

## SUPPLEMENTARY METHODS

### Detailed clinical studies

Blood cell counts, routine blood biochemical analysis, clotting measurement, thyroid function testing, autoantibody screening, and treponemal serology were performed. Levels of anti-glutamic decarboxylase, anti-human T-lymphotropic virus-I antibodies, anti-human immunodeficiency virus antibodies, ceruloplasmin, copper, very-long-chain fatty acids, vitamin B12 and folic acid were measured. Needle electromyography (abductor digiti minimi, spinalis thoracis and tibialis anterior muscles), surface antidromic sensory (sural and median nerves) and orthodromic motor (median, tibial or peroneal nerves) nerve conduction studies were obtained in all patients with an electromyography machine (Synergy, CareFusion, San Diego, CA 92130, EEUU). Genetic testing of the most strongly affected patients (II:3 and II:5) was performed by Sanger sequencing and MLPA for the most common causes of spastic paraparesis (SPG3, SPG4, SPG10 and SPG11), Sanger sequencing for X-linked adrenomyeloneuropathy (*ABCD1*, together with analysis of very-long-chain fatty acid levels), as well as dynamic expansion analysis in genes associated to spinocerebellar ataxia (1, 2, 3, 6, 7, 8, 10, 14, and 17), DRPLA, and Friedrich's ataxia, with negative outcome.

### Radiological assessment

In patients II:2, II:3, II:5, III:4 and III:5, a brain and spinal cord MRI scan was performed. Brain MRI protocol included T1 and T2 weighted, fluid attenuated inversion recovery (FLAIR) and diffusion- weighted imaging (DWI) sequences in the sagittal and axial planes. Spinal cord MRI protocol included T1 and T2 weighted and short tau inversion recovery (STIR) sequences in the sagittal and axial planes. All the exams were obtained indistinctly on a 1.5T or 3T scanner. MRI examinations were read by an unblinded neuroradiologist. A systematic evaluation of periventricular signal changes, the periventricular rim of decreased T2 signal and increased T1 signal, brainstem enhancement or signal change, brainstem atrophy, spinal cord atrophy, spinal

cord enhancement and signal change, cerebellar enhancement and signal change, "tadpole atrophy" of the brainstem with relative sparing of pons, ependymal nodularity and thalamic or basal ganglia signal abnormality was performed.

Short and long TE single voxel 1H MR spectroscopy (PRESS sequence, short TE=30ms, long TE=136ms) was performed for patients II:2, II:3, II:5 and III:2. The voxel was positioned on a three-dimensional FLAIR image centered in the area of signal and morphologic abnormality in the medulla/ cord-medulla junction. These exams were all acquired on a 3T scanner.

**Molecular studies**

Blood samples were obtained with informed consent. Genomic DNA was extracted from peripheral blood using standard methods. WES was performed on two patient DNA samples using the SureSelect XT Human All Exon V5 50 Mb kit (Agilent) for DNA capture and sequencing with the HiSeq 2000 Platform (Illumina) at CNAG (Centre Nacional d'Anàlisi Genòmica, Barcelona). We prioritized non-synonymous coding variants that had a frequency lower than 0.001 in the ExAC, 1000 genomes, and gnomAD databases and were present in both patients. Candidate variants were validated and tested for cosegregation in all available family members by Sanger sequencing. The logarithm of odds (LOD) score was calculated with the MERLIN package using the variant genotype as entry data.

Human GFAP full-length cDNA (NM_002055.4) was amplified by PCR excluding the stop codon using an MGC Human GFAP Sequence-Verified cDNA vector as a template (MHS6278-202757583, Dharmacon™) with primers incorporating EcoRI (forward) and BamHI (reverse) restriction sites. cDNA was cloned into the pEGFP-N3 vector (Clontech) upstream of the EGFP cDNA sequence, generating a GFAP-EGFP fusion cDNA in which EGFP was fused to the C-terminus of GFAP. A recurrent Alexander disease mutation used as a positive control (p.Arg239Cys) and the p.Gly18Val mutation were introduced through site-directed mutagenesis (QuikChange™ kit, Agilent) using the wild-type GFAP-EGFP fusion vector as a template. All constructs were checked by Sanger sequencing.

The U-251 MG human astrocytoma cell line (Sigma-Aldrich) was maintained in DMEM (Gibco, Life Tech.) supplemented with 10% FBS, 100 U/ml penicillin, and 100 µg/mL streptomycin in a cell incubator at 5% CO2, 25°C. Cells were seeded into 6-well plates to 90% confluence in 24 h. Transfections were performed using 1 or 4 µg of GFAP-EGFP fusion vector (wild type (WT), p.Arg239Cys or p.Gly18Val) and 3 µl Lipofectamine 2000 per well (Life Tech.) diluted in Opti-MEM I medium (GibcoTM-ThermoFisher). After transfection for 3 hours, cells were cultured for 24 or 48 h and then fixed in 4% PFA. For colocalization studies, immunocytochemistry was performed using Polyclonal Rabbit Anti-Glial Fibrillary Acidic Protein Z0334 antibody (1/500, Dako) and Goat Anti-Rabbit IgG Alexa Fluor 555 A-21428 (1/1000, Dako). DAPI was used to stain cell nuclei.

Confocal microscopy images were acquired with a Leica TCS SL laser scanning confocal spectral microscope using a 63x objective. To analyse GFAP networks and aggregates in detail, a 4x zoom was used. Cell area was determined with ImageJ via analysing GFAP-EGFP fluorescence by using the “Analyse particles” tool. A minimum number of 40 cells was analysed per genotype and condition. Statistical significance was evaluated by a one-sided ANOVA test, followed by post hoc Tukey’s test.

**Supplemental Table 1. Clinical Findings**

| | I:2 | II:2 | II:3 | II:5 | III:4 | III:5 |
|---|---|---|---|---|---|---|
| Sex | F | F | F | F | M | M |
| Age of onset | NA | NA | 46 | 17 | 10 | 9 |
| Age of diagnosis | 73 | 49 | 50 | 40 | 16 | 12 |
| Nystagmus | + | + | + | + | + | + |
| Spasticity | - | - | + | + | + | + |
| Hyperreflexia | + | + | + | + | + | + |
| Babinski sign | + | + | + | + | + | + |
| Hoffman sign | - | + | + | + | + | + |
| Gait abnormality | + | + | + | + | + | + |
| Weakness | - | - | + | + | + | + |
| Bladder dysfunction | - | - | + | + | - | - |
| Scoliosis | - | + | + | - | + | + |
| Palatal tremor | - | - | - | - | - | - |
| Dysarthria / dysphagia | - | - | - | - | - | - |
| Dysautonomia | - | - | - | - | - | - |

F: Female, M: Male. + : Presence of the feature. - : Absence of the feature. NA: Not Available

**Supplemental Table 2. Radiological Findings**

| Case | **II:2** | **II:3** | **II:5** | **III:4** | **III:5** |
|---|---|---|---|---|---|
| White Matter Changes | No | No | No | No | No |
| Periventricular Rim (T2 signal decreased/ T1 signal increased) | No | No | No | No | No |
| Brainstem Pial FLAIR Signal Change | Medulla | Medulla and midbrain (+) | Medulla | Medulla | Medulla |
| Brainstem Atrophy | No | Medulla Mild Atrophy | Medulla Mild Atrophy | Medulla Mild Atrophy | Medulla |
| Spinal Cord Signal Change | Cervical | Cervical | Cervical and Dorsal | Cervical | Yes |
| Spinal Cord Atrophy | No | Cervical and Dorsal | Cervical and Dorsal | Cervical and Dorsal | Cervical and dorsal |
| Tadpole Atrophy (*) | No | Yes | Yes | Yes | Yes |
| Enhancement | Mild Medulla | Mild Medulla | No | Mild Medulla | Mild Medulla |
| Middle Cerebellar Peduncle Involvement | No | No | No | No | No |
| Cerebellar / dentate findings | Anomaly of venous draining | No | No | No | No |
| Ependymal Nodularity | No | No | No | No | No |
| Thalamic / Basal Ganglia abnormality | No | No | No | No | No |

* : Atrophy of medulla and cervical cord with sparing pons

+ : Posterior periaqueductal

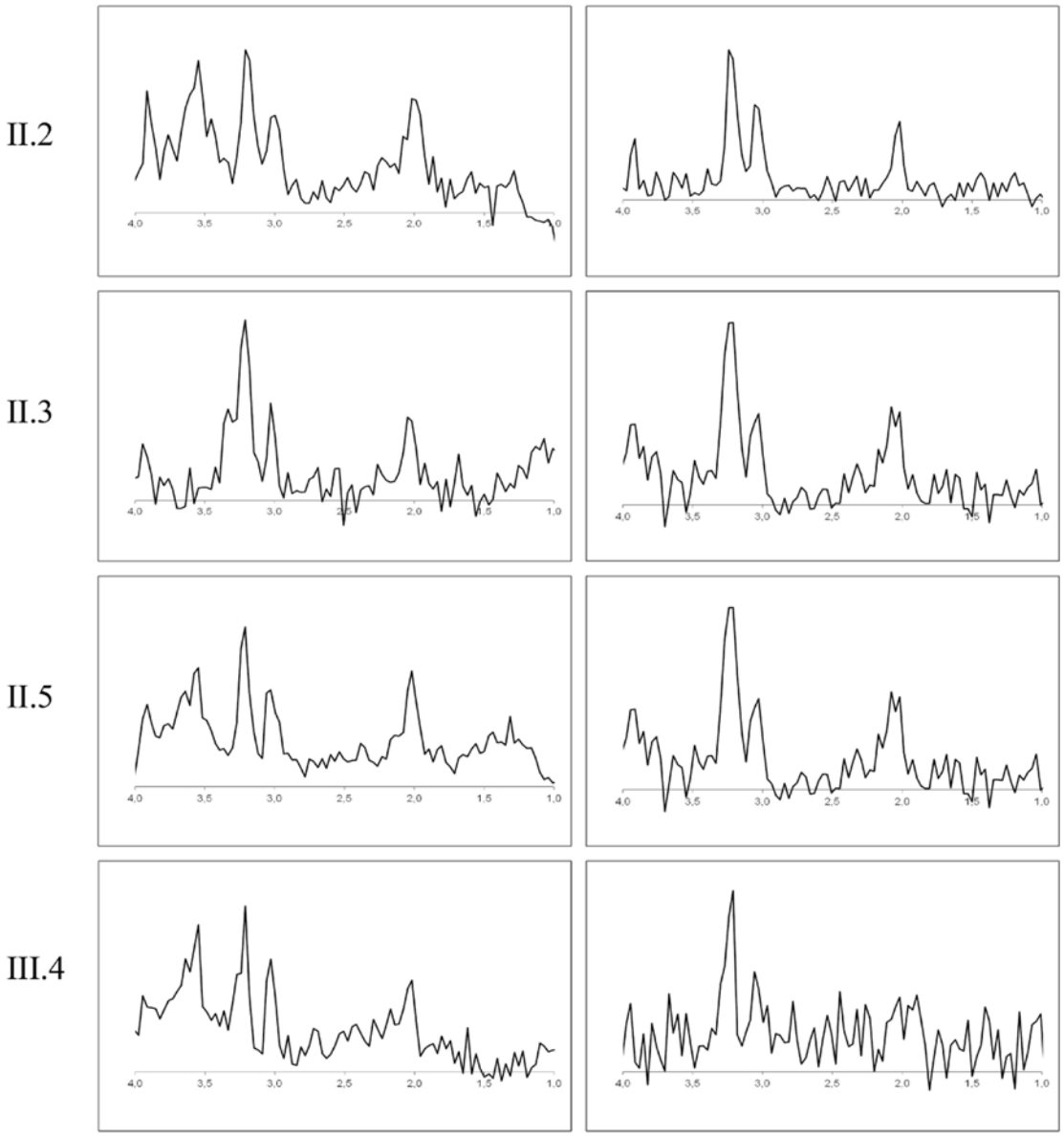


**Supplemental Image 1: Proton MRS of Patients II:2, II:3, II:5, III:4 in the medulla-cord junction.** First column: short TE (30ms). Second column: long TE (136ms).

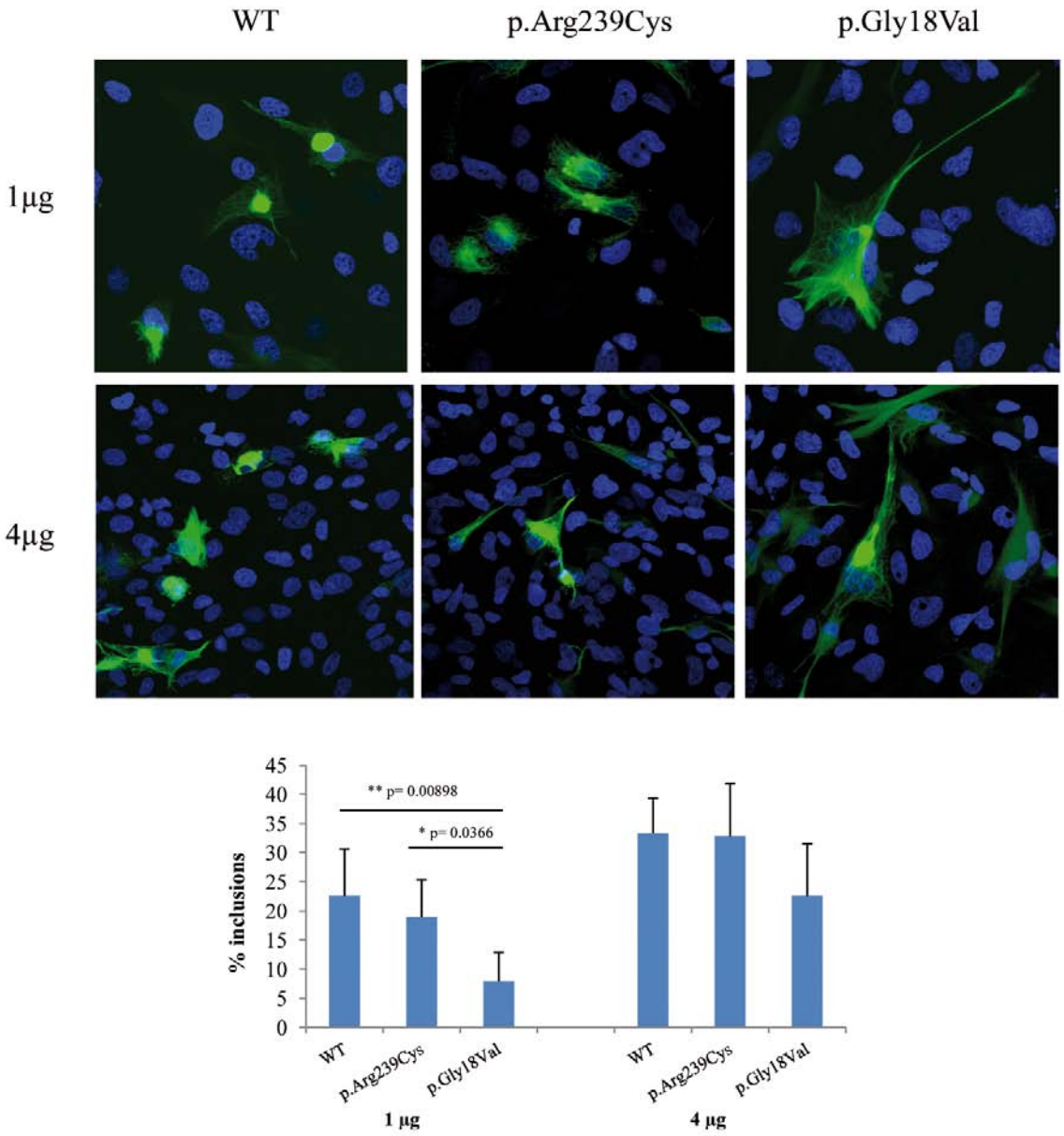


**Supplemental Figure 2: GFAP inclusions or aggregates in U251-MG transfected cells**. In blue: DAPI staining; Green: EGFP fluorescence. Transfection was carried out with 1 or 4 µg of plasmid per well (6-well plate), and pictures were taken 48h after. A) While WT and p.Gly18Val –transfected cells show GFAP-EGFP protein inclusions, p.Arg239Cys-transfected cells (positive control of aggregation) show the presence of little dot-like clumps or aggregates.. B) Quantification of GFAP inclusions in transfected U251-MG cells. Data are expressed as mean ± s.d. One-way ANOVA was performed, followed by post-hoc Tukey's test.